Molecular Electroluminescence

DOI: 10.1002/ange.201301209

Fluorescence and Phosphorescence of Single C_{60} Molecules as Stimulated by a Scanning Tunneling Microscope**

*Guangjun Tian and Yi Luo**

As a promising method for the study of single molecules by means of optical spectroscopic measurements, molecular electroluminescence (EL) stimulated by a scanning tunneling microscope (STM) has attracted great research interest during the last decade.[1] It is a sophisticated experimental approach that requires state-of-the-art instrumentation. Unlike STM-induced photon emission from a noble-metal surface as a result of the radiative decay of localized surface plasmons (LSPs),[2] the formation of electron–hole pairs is essential for the observation of EL from single molecules. Such an electron–hole pair can be generated when an electron is excited to the virtual orbital of the molecule. The recombination of the electron–hole pair then leads to the emission of photons with a spectral distribution determined by the electronic structure of the molecule. In an STM tunneling junction, such an electron–hole pair is normally generated through the excitation of the molecule by the tunneling electrons. Recent experiments[1e,f,3] and theoretical studies[4] indicated that the LSPs formed between the STM tip and the substrate could also facilitate or even dominate the generation of electron–hole pairs.

Among the very few experimental observations of EL from single molecules in an STM, the spectra of C_{60} molecules[1c] show the richest features. It was found that the spectral profile of C_{60} could be changed drastically under different measurements. These changes were first attributed to the vibronic structures of the fluorescence and phosphorescence.[1c] However, the assignment of the spectral features is not straightforward and has actually been changed over the years. At first, the two well-separated emission bands in the observed phosphorescence were assumed to correspond to photon emission from two triplet excited states, T_1 and T_2, of C_{60}.[1c] However, this assumption is against the well-established Kasha's rule, which states that photon emission of a given multiplicity can occur only from the lowest excited state of that multiplicity.[5] In a later study by the same research group,[1e] a possible correlation between the spectral changes and the LSPs was observed, but its origin was not identified. Moreover, the previously reported phosphorescence spectra of C_{60} were reinterpreted as fluorescence spectra, although contributions from phosphorescence could not be completely ruled out. It is clear that proper theoretical modeling is needed to clarify the confusion and to demonstrate the feasibility of STM-induced EL as a tool for identifying molecules at the single-molecule level.

The EL from C_{60} molecules is complicated not only by their large size but also by two difficulties for theoretical modeling. The first is the modeling of the vibronic couplings involved in both fluorescence and phosphorescence, since the first excited singlet and triplet states of C_{60} are dipole-forbidden states. The other difficulty is the strong impact of the local plasmonic excitations on the spectral profiles. In this study, we developed a general theoretical model based on the density-matrix method to include both Condon and non-Condon vibronic contributions to simulate the STM-induced EL of single C_{60} molecules (see the Supporting Information for the theoretical framework). We identified the unique spectral fingerprint of the fluorescence and phosphorescence of a C_{60} molecule as stimulated by an STM. The effects of Condon and non-Condon vibronic coupling, the tunneling-electron-induced excitations and the localized-surface-plasmon-induced excitations were examined carefully. The calculated spectra nicely reproduced the corresponding experimental spectra; thus, we were able to identify the origins of the EL and to correctly assign the rich spectral features.

A schematic diagram of the processes that can take place when a C_{60} molecule is confined inside an STM is shown in Figure 1a. The ground state of C_{60} is a singlet state (S_0). The molecule can be promoted to the excited states through two possible excitation processes, namely, electron-tunneling-induced excitation and plasmon-assisted excitation. The former requires the presence of both the highest occupied molecular orbital (HOMO) and the lowest unoccupied molecular orbital (LUMO) of the molecule in the bias window. Electrons can tunnel into the LUMO and tunnel out from the HOMO simultaneously, which leaves the molecule in one of its excited states. Depending on the spin multiplicity of the resulting state, the molecule may be in either the first singlet excited state (S_1) or the first triplet excited state (T_1). Both states can then emit light to generate fluorescence (from S_1) or phosphorescence (from T_1). Moreover, the presence of the plasmon induced by electron tunneling can lead to

[*] G. Tian, Prof. Dr. Y. Luo
Heifei National Laboratory for Physical Science at the Microscale
University of Science and Technology of China
Heifei, 230026 Anhui (P. R. China)
and
Theoretical Chemistry and Biology, School of Biotechnology
Royal Institute of Technology
10691 Stockholm (Sweden)
E-mail: luo@kth.se

[**] This research was supported by the Major State Basic Research Development Programs (2010CB923300), the National Natural Science Foundation of China (20925311), the Swedish Research Council, and the Göran Gustafsson Foundation for Research in Natural Sciences and Medicine. The simulations were performed with resources provided by the Swedish National Infrastructure for Computing (SNIC) at PDC and NSC.

Supporting information for this article is available on the WWW under http://dx.doi.org/10.1002/anie.201301209.

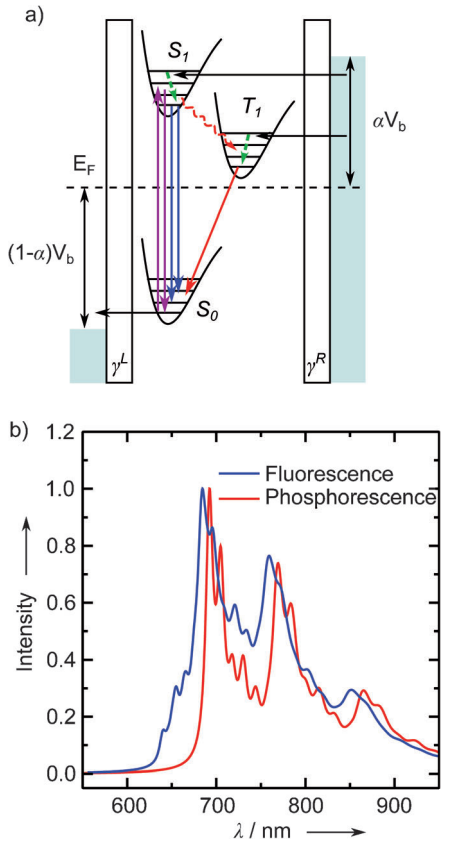

Figure 1. a) Schematic diagram of the energetic states of the molecule in the bias-voltage window. The possible excitation and photon-emission processes are also shown as arrows. The nonradiative decay processes are shown as dashed arrows. b) Calculated fluorescence (blue) and phosphorescence spectra (red) of a C_{60} molecule in free space.

resonant excitation and emission as shown by violet arrows. Owing to the dipole- and spin-selection rule, plasmon-assisted excitation and photon emission can occur between the singlet states.

We carried out density functional theory (DFT) calculations to obtain the optimized geometries and vibrational frequencies of C_{60} in the three electronic states. It is well-established that the major contribution to the fluorescence ($S_1 \rightarrow S_0$) comes from the non-Condon effect, such as Herzberg–Teller (HT) coupling.[6] We calculated the nuclear-coordinate-dependent transition dipole moment numerically for all vibrational modes to accurately account for the HT contributions to the fluorescence spectrum. The vibronic coupling in the phosphorescence spectrum ($T_1 \rightarrow S_0$) was analyzed by the same "displaced-oscillator" approach adopted by Cepek et al.,[7] which is an efficient way to account for the effect of Jahn–Teller distortions on the T_1 state. By this approach, the vibronic contributions can then be determined from the square of the overlaps of the displaced harmonic oscillators, that is, the Franck–Condon (FC) factors. The most active modes in the fluorescence and phosphorescence are summarized in the Supporting Information, which also includes a detailed description of the method used to calculate the displacement vectors as well as the FC and HT factors. The calculated free-molecule fluorescence and phosphorescence spectra are shown in Figure 1 b. The two spectra have very similar profiles; they exhibit two main emission peaks with several vibronic side bands. The similarity arises because the most active modes in the $S_1 \rightarrow S_0$ and $T_1 \rightarrow S_0$ transitions are close in energy and have similar displacement vectors (see Table S1 in the Supporting Information). The main peaks of the two spectra differ from each other by only 8 nm, which makes them very difficult to distinguish experimentally. The most visible difference between them seems to be the shoulder that occurs in the fluorescence spectrum but not in the phosphorescence spectrum at the higher-energy side of the spectrum. The observation that the rich vibronic structure in the phosphorescence spectrum of the C_{60} molecule results from one triplet state, T_1, and not from two triplet states (T_1 and T_2), as claimed in a previous experimental study, is very important.[1c] In other words, the Kasha's rule holds for the phosphorescence of C_{60}.

We could now simulate the EL spectra under plasmonic excitation on the basis of the density-matrix approach by considering all vibrational modes involved. In recent experiments, Rossel et al. recorded two different EL spectra of C_{60} under different conditions with respect to the STM tip (the two measured spectra are reproduced in Figures 3 and 4 b).[1e] They found that the measured spectra had similar peak positions but very different emission profiles, possibly as a result of the involvement of the plasmonic excitation, as was clearly observed for tetraphenylporphyrin molecules.[1f] To verify these observations, we took the two experimentally measured surface-plasmon modes (shown in Figure 2 a)[1e] as the input to simulate the spectra under plasmonic excitation. The measured surface plasmons were fitted by Gaussian functions in the frequency domain. The resulting Gaussian functions were then Fourier transferred to the time domain as Gaussian pulses.[8] The Gaussian pulses were characterized by the resonant frequency ($\hbar\omega$), the duration (τ), and the field strength (E_0). The resonant frequency and duration can be derived from the peak position and the half-width at half-maximum (HWHM) of the experimental plasmon modes, respectively. The direct calculation of the field strength is still a challenging issue. In the present study, we treated the field strength as an adjustable parameter and examined in detail the dependence of the EL spectrum on the field strength. The measured surface-plasmon modes and the corresponding pulse structure in the time domain are shown in Figure 2 a,b. The plasmon mode with an energy maximum at the high-energy side is named mode I, whereas another with an energy maximum at the low-energy side is called mode II.

The calculated fluorescence under the two experimental plasmon modes is given in Figure 2 c. The calculated EL spectra without the inclusion of the surface-plasmon excitation (with $E_0 = 0\ \mathrm{V\,m^{-1}}$) are also shown to directly demonstrate the effect of plasmon excitation on the EL spectrum. As the plasmon strength increases, not only is the overall intensity of the EL spectra enhanced, but the spectral profile also shows noticeable changes, in particular for mode I. Although they are very different in terms of the overall spectral profile, one common feature shared by both sets of

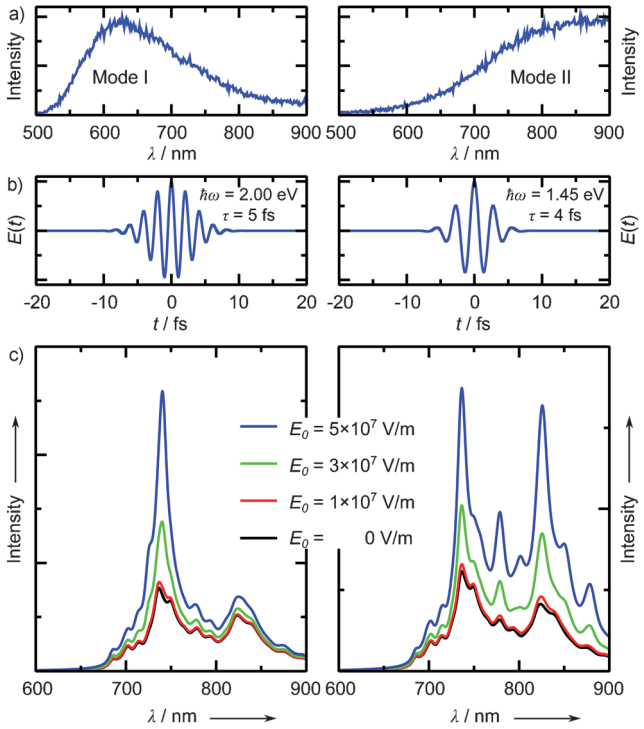

Figure 2. a) Two plasmon modes measured in experiments (Ref. [1e]). b) Corresponding pulse shapes of the two plasmon modes. The resonant energy and duration of the two pulses are 2.00 eV, 5.0 fs (mode I) and 1.45 eV, 4.0 fs (mode II). c) Calculated EL spectra of a C_{60} molecule as a function of the strength of the surface-plasmon field (left: mode I, right: mode II). The high-energy shoulders in the calculated EL spectra are highlighted. HWHM = 100 cm^{-1}.

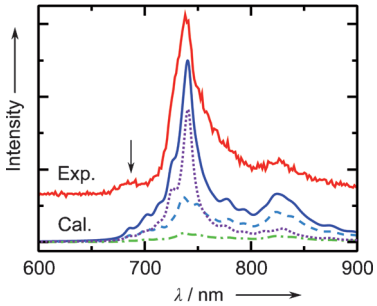

Figure 3. Measured (Ref. [1e]) and calculated EL spectra under the excitation of a surface-plasmon mode of a C_{60} molecule ($\tau = 5.0$ fs, $\hbar\omega = 2.00$ eV, $E_0 = 5.0\times10^7$ V m^{-1}, HWHM = 100 cm^{-1}). The surface-plasmon-assisted emission (dotted line), the spontaneous emission (dashed line), and the electron-tunneling-induced emission (dashed–dotted line) are also shown. The measured spectrum is shifted vertically for comparison.

EL spectra is that the shoulder at the high-energy side is always present, regardless of the shape and the strength of the plasmon excitations. This shoulder does not occur in the phosphorescence spectrum and can be used as a fingerprint to distinguish the two different processes. It can thus be concluded that the two experimental spectra for modes I (shown in Figure 3) and II (Figure 4b)[1e] result from plasmon-assisted fluorescence and phosphorescence, respectively. In

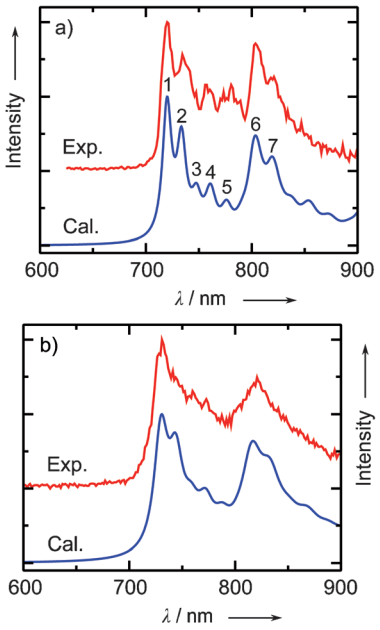

Figure 4. Comparison of the measured EL spectra (Ref. [1c] and Ref. [1e]) and the calculated STM-induced phosphorescence with different values of HWHM: a) HWHM = 100 cm^{-1}; b) HWHM = 150 cm^{-1}. The measured spectra are shifted vertically for comparison.

the following we compare the simulated and experimental spectra in detail.

In general, one can see that mode I has a strong effect on the main peak of the EL spectrum (Figure 2). With a high plasmon strength, for example, when $E_0 = 5.0\times10^7$ V m^{-1}, the resulting EL spectrum exhibits only one strong emission peak with several side peaks and resembles the corresponding experimental spectrum very well (Figure 3). Different contributions to the total photon-emission process are also given in Figure 3. Apparently, the EL is dominated by the plasmon-assisted emission, which leads to absolutely dominant spectral features. When the calculated and experimental spectra are compared, not only does the overall spectral profile fit well, but also the small details, such as the occurrence of high-energy emission peaks marked by the arrow in Figure 3.

The first phosphorescence spectrum of C_{60} molecules under scanning tunneling microscopy was reported in 2005 (Figure 4a).[1c] The double-band structure, with peaks located at 720 and 803 nm, was attributed to emission from the first (T_1) and second (T_2) triplet states. A similar spectrum was observed later by the same research group (Figure 4b), but was assigned to the fluorescence affected by plasmonic excitations.[1e] The absence of the high-energy shoulders in both spectra suggests that these spectra are not likely to be due to fluorescence. In Figure 4, we compare our calculated phosphorescence spectra with the two experimental spectra. The agreement between the spectra is very good, which indicates that phosphorescence can indeed be a possible product of the electroluminescence of C_{60} molecules under scanning tunneling microscopy. The difference between the two experimental spectra is caused by different experimental resolutions.

This excellent agreement enabled us to confirm that the triplet-to-singlet transition ($T_1 \rightarrow S_0$) is responsible for the measured phosphorescence spectra. The double-band structure in the observed EL spectra is the result of vibronic coupling. The assignment of the emission peaks (labeled in Figure 4a) on the basis of the calculated phosphorescence is given in Table 1. The high-energy band, which consists of two split peaks and a series of vibronic side bands, contains the fundamental (0,0) transition, the (0,1) and (0,2) transition of the JT-active $h_g(1)$ mode, the (0,1) transition of the $g_u(3)$ mode, and the (0,2) overtones of the $h_g(1)$ and $g_u(3)$ modes. The low-energy band has a shape similar to that of the first band. Its first emission peak consists of the (0,1) transition of modes $t_{1u}(4)$ and $g_g(6)$. Two (0,2) transitions, $^1h_g(1)^1t_{1u}(4)$ and $^1h_g(1)^1g_g(6)$, are the main contributors to the adjacent emission peak.

Table 1: Assignment of the peaks in the phosphorescence spectrum ($T_1 \rightarrow S_0$) as labeled in Figure 4a.

Peak	Position [nm]	Transition	Assignment
1	720	(0,0)	–
2	734	(0,1)	$^1h_g(1)$
3	748	(0,2)	$^2h_g(1)$
4	761	(0,1)	$^1g_u(3)$
5	776	(0,2)	$^1h_g(1)^1g_u(3)$
6	804	(0,1)	$^1t_{1u}(4)$ and $^1g_g(6)$
7	819	(0,2)	$^1h_g(1)^1t_{1u}(4)$ and $^1h_g(1)^1g_g(6)$

In summary, we have presented a systematic study on the EL from single C_{60} molecules in an STM. By combining the density-matrix approach with first-principles calculations, we successfully reproduced the measured EL spectra and were able to assign the measured spectra unambiguously. It was found that EL from C_{60} molecules can be generated either from the singlet state (fluorescence) or the triplet state (phosphorescence), depending on the experimental conditions. The high-energy shoulder in the EL spectrum can be used as the spectral fingerprint to distinguish the two processes. The surface plasmonic excitations can significantly modify the fluorescence spectrum, but not the phosphorescence spectrum. Our study demonstrates yet again the power of theoretical modeling for gaining an understanding of the very complicated processes involved in the EL of molecules in an STM.

Experimental Section

Computational details: The electronic structure and the vibrational frequencies were obtained by DFT and time-dependent DFT calculations with a hybrid B3LYP functional[9] and a 6-31G basis set, as implemented in Gaussian 09 software.[10] The calculated vibrational frequencies were scaled with a constant vibrational-frequency scaling factor of 0.96[11] to take into account the anharmonicity and the systematic error of the model. The optimized geometries (given in the Supporting Information) and the vibrational normal modes were then used to compute the FC and HT factors. To take into account the Jahn–Teller distortion, a constant scale factor (0.7), as used by Cepek et al. in their study of the electron energy loss spectrum of C_{60},[7] was introduced to scale the computed displacement parameter of all JT-active h_g modes. The derivatives of the transition dipole moment with respect to the normal modes were evaluated numerically at the optimized geometry of S_1. The FC and HT factors were calculated with our DynaVib software.[12]

The equation of motion of the density matrix was solved by using a fourth-order Runge–Kutta method. Because of the large number of vibrational states involved in the calculations, the stationary population of the molecule under the excitation of tunneling electrons was chosen as the starting point. The radiative and nonradiative lifetimes were set to 2 ns and 2 ps, respectively. The bare tunneling rates from the STM tip (γ^L) and the substrate (γ^R) to the molecule are 4.10 and 0.41 μeV, respectively. The simulations were performed at 50 K, which is the same temperature as that used for the experiments.[1c,e] The line-shape broadening caused by dephasing is described by the Lorentzian function with the given HWHM. The simulations were carried out with a bias voltage (V_b) of −3.0 V. The bias coupling (α) was 0.5. For the sake of better presentation, the calculated EL spectra shown herein were calibrated with respect to the experimental maximum. By using mode I (Figure 2) as an example, we examined the influence of the response of the detectors (as measured by Schneider et al.[13]) and found that it only led to a minor change in the overall profile of the surface-plasmon mode.

Received: February 11, 2013
Published online: March 28, 2013

Keywords: electroluminescence · fullerenes · scanning tunneling microscopy · single-molecule studies · vibrational spectroscopy

[1] a) X. H. Qiu, G. V. Nazin, W. Ho, *Science* **2003**, *299*, 542 – 546; b) Z. C. Dong, X. L. Guo, A. S. Trifonov, P. S. Dorozhkin, K. Miki, K. Kimura, S. Yokoyama, S. Mashiko, *Phys. Rev. Lett.* **2004**, *92*, 086801; c) E. Ćavar, M.-C. Blüm, M. Pivetta, F. Patthey, M. Chergui, W.-D. Schneider, *Phys. Rev. Lett.* **2005**, *95*, 196102; d) S. W. Wu, G. V. Nazin, W. Ho, *Phys. Rev. B* **2008**, *77*, 205430; e) F. Rossel, M. Pivetta, F. Patthey, W.-D. Schneider, *Opt. Express* **2009**, *17*, 2714 – 2721; f) Z. C. Dong, X. L. Zhang, H. Y. Gao, Y. Luo, C. Zhang, L. G. Chen, R. Zhang, X. Tao, Y. Zhang, J. L. Yang, J. G. Hou, *Nat. Photonics* **2010**, *4*, 50 – 54; g) C. Chen, P. Chu, C. A. Bobisch, D. L. Mills, W. Ho, *Phys. Rev. Lett.* **2010**, *105*, 217402.
[2] R. Berndt, J. K. Gimzewski, P. Johansson, *Phys. Rev. Lett.* **1991**, *67*, 3796 – 3799.
[3] N. L. Schneider, R. Berndt, *Phys. Rev. B* **2012**, *86*, 035445.
[4] G. Tian, J.-C. Liu, Y. Luo, *Phys. Rev. Lett.* **2011**, *106*, 177401.
[5] M. Kasha, *Discuss. Faraday Soc.* **1950**, *9*, 14 – 19.
[6] a) F. Negri, G. Orlandi, F. Zerbetto, *J. Chem. Phys.* **1992**, *97*, 6496 – 6503; b) F. Negri, G. Orlandi, F. Zerbetto, *J. Phys. Chem.* **1996**, *100*, 10849 – 10853.
[7] C. Cepek, A. Goldoni, S. Modesti, F. Negri, G. Orlandi, F. Zerbetto, *Chem. Phys. Lett.* **1996**, *250*, 537 – 543.
[8] G. Tian, Y. Luo, *Phys. Rev. B* **2011**, *84*, 205419.
[9] a) C. Lee, W. Yang, R. G. Parr, *Phys. Rev. B* **1988**, *37*, 785 – 789; b) A. D. Becke, *J. Chem. Phys.* **1993**, *98*, 5648 – 5652; c) A. D. Becke, *J. Chem. Phys.* **1993**, *98*, 1372 – 1377.
[10] Gaussian 09, Revision A.02, M. J. Frisch et al., Gaussian, Inc., Wallingford CT, **2009**.
[11] A. P. Scott, L. Radom, *J. Phys. Chem.* **1996**, *100*, 16502 – 16513.
[12] DynaVib, Version 1.0, G. Tian, S. Duan, W. Hua, Y. Luo, Royal Institute of Technology, Sweden, **2012**.
[13] N. L. Schneider, F. Matino, G. Schull, S. Gabutti, M. Mayor, R. Berndt, *Phys. Rev. B* **2011**, *84*, 153403.

